

# Comparative Efficiency Measurement of UAV Propellers Using a Microcontroller-Based Test Bench

**Erwan Eko Prasetyo**

Sekolah Tinggi Teknologi Kedirgantaraan, Bantul, Special Region of Yogyakarta, Indonesia  
erwan.eko@sttkd.ac.id (corresponding author)

**Erwhin Irmawan**

Sekolah Tinggi Teknologi Kedirgantaraan, Bantul, Special Region of Yogyakarta, Indonesia  
erwhin.irmawan@sttkd.ac.id

**Gaguk Marausna**

Sekolah Tinggi Teknologi Kedirgantaraan, Bantul, Special Region of Yogyakarta, Indonesia  
gaguk.marausna@sttkd.ac.id

**Ikbal Rizki Putra**

Sekolah Tinggi Teknologi Kedirgantaraan, Bantul, Special Region of Yogyakarta, Indonesia  
ikbal.rizki@sttkd.ac.id

**Hendriana Helda Pratama**

Sekolah Tinggi Teknologi Kedirgantaraan, Bantul, Special Region of Yogyakarta, Indonesia  
hendriana.helda@sttkd.ac.id

**Fadhli Atha Hidayat**

Sekolah Tinggi Teknologi Kedirgantaraan, Bantul, Special Region of Yogyakarta, Indonesia  
21021126@students.sttkd.ac.id

*Received: 21 October 2025 | Revised: 15 November 2025 | Accepted: 1 December 2025*

*Licensed under a CC-BY 4.0 license | Copyright (c) by the authors | DOI: <https://doi.org/10.48084/etasr.15694>*

## ABSTRACT

Optimizing small-scale electric propulsion systems is essential for improving Unmanned Aerial Vehicle (UAV) performance. However, the complexity and specialized nature of commercial test equipment remain a significant barrier. This paper details the design, fabrication, and validation of an accessible, microcontroller-based instrument capable of comprehensive performance characterization. The system integrates an ESP32 microcontroller to simultaneously measure mechanical thrust, electrical power consumption, and exit airflow velocity. To demonstrate its analytical capabilities, the instrument was used to conduct a comparative study on three 10×5-inch propellers fabricated using different methods: commercial injection molding, silicone mold casting, and 3D printing. The results revealed significant performance variations, with the developed instrument successfully measuring total propulsive efficiencies ranging from 18% to a peak of 30%. The commercial propeller was identified as the most efficient. This study validates the developed test bench as an effective and accessible tool for detailed analysis and the optimization of electric propulsion systems.

*Keywords-propeller efficiency; thrust stand; performance evaluation; UAV; electric propulsion*

## I. INTRODUCTION

The Unmanned Aerial Vehicle (UAV) industry is transforming many global sectors [1, 2], yet the full potential of

these platforms is constrained by the performance limitations of on-board electric propulsion systems [3]. As a core technology, the electric propulsion systems, which are integrated assemblies consisting of a motor, an Electronic Speed

Controller (ESC), and a propeller, govern critical capabilities [1]. Key performance indicators, such as flight endurance and payload capacity, are directly dictated by the efficiency of the powertrain. Consequently, electric propulsion system optimization has become a central focus of aerospace research, often using advanced methodologies to navigate complex trade-offs [4].

Successful optimization requires accurate performance data. While computational models like Blade Element Momentum Theory (BEMT) provide powerful predictive tools, their efficacy depends on empirical validation against real-world measurements [5]. Therefore, precise experimental characterization using dedicated test stands is significant for UAV development [6, 7]. Authors in [8, 9] present various instrument designs, from pendulum-based systems for different thrust ranges to advanced six-degree-of-freedom (6-DOF) stands for measuring critical off-axis forces [10]. These designs are often tailored to specific propulsion scales, ranging from large propeller rigs to sensitive balances for millinewton-level micro propulsion [11, 12], with some advancements integrating machine learning to improve accuracy [13]. Despite its importance, the field of experimental validation faces several persistent challenges. High-fidelity commercial test instruments are often very costly and inaccessible to many academic and research institutions [14]. In response, numerous custom-built test stands have been developed; however, these approaches often suffer from limitations, including an exclusive focus on single metrics, such as thrust or a lack of integrated sensor suites, and automated data acquisition systems, necessary for a holistic efficiency analysis [7, 15]. Alternative indirect methods, such as force probes measuring the plume's momentum transfer, have also been developed and validated with limited success [16].

To address these shortcomings, this study presents the design, fabrication, and empirical validation of an accessible, microcontroller-based instrument for comprehensive propulsion system analysis. The main contribution of the present study lies in design, fabrication, and validation of a unified test stand that integrates a load cell for thrust measurement, a wattmeter for electrical power consumption, and an anemometer for exit airflow velocity, all synchronized by an ESP32 microcontroller. This integrated approach facilitates the direct calculation of the total propulsive efficiency ( $\eta_{total}$ ). To demonstrate its analytical utility and validate its accuracy, the instrument is utilized to conduct a comparative study on three propellers of identical geometry fabricated using different manufacturing methods. This study, thus presents and validates an accessible engineering tool and delivers novel empirical data on how fabrication techniques impact system efficiency.

## II. METHODOLOGY

This study employed a structured quantitative experimental design, which includes:

- Design and fabrication of a robust, custom-built measurement instrument.

- Instrument utilization to conduct a comparative performance analysis of three propeller types.
- Collected data analysis to characterize and validate system performance.

The research workflow is summarized in Figure 1.

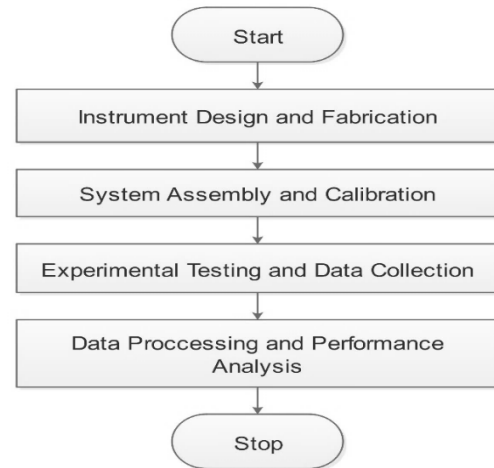


Fig. 1. Flowchart of the research methodology.

### A. Instrument Design and Fabrication

The feasibility of custom-built, modular test benches has been demonstrated [17]. The core of this research lies in a custom test stand engineered for static testing of small-scale electric propulsion systems. The mechanical layout was conceptualized for high structural rigidity to minimize vibration errors, inspired by the Tyto Robotics Series 1585 test stand [18]. The entire structure was first modeled in detail using CAD software, as shown in Figure 2.

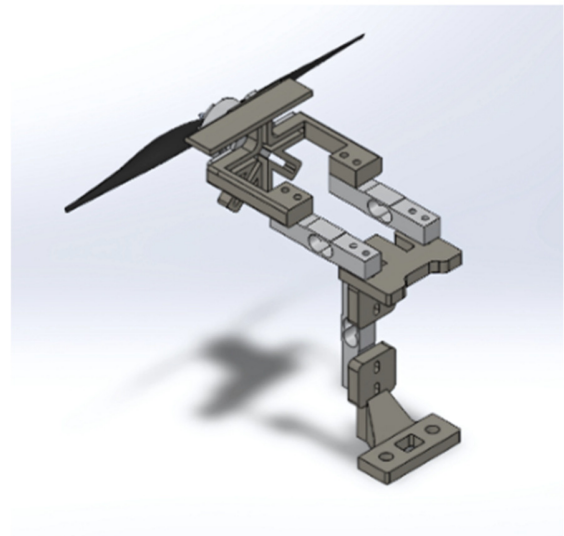


Fig. 2. Detailed CAD model of the integrated thrust stand.

Following the design phase, the structure was fabricated using Fused Deposition Modeling (FDM). Polylactic Acid (PLA) filament was chosen as the build material for its optimal balance of high rigidity, ease of customizability, and ease of fabrication, supporting the instrument's accessibility. The final frame was engineered with precision tolerances to securely house the BLDC motor and load cell sensor. This design ensured precise axial alignment between the propeller and sensor, a critical factor for accurate, on-axis thrust measurement. The fabricated test bench frame, constructed from FDM PLA, has dimensions of 15.37 cm × 7.64 cm × 19.10 cm. This frame was then securely mounted on a rigid wooden base plate. The addition of this wooden base was crucial to provide a high-inertia, stable foundation. This foundation effectively dampens ambient vibrations and ensures

that the forces captured by the load cell are a direct result of the propulsion system's thrust.

The FDM design provides ample physical clearance for propellers larger than the 10×5-inch models used in this study. However, the practical limit of the current configuration is defined by the selected motor, not the frame. The A2212 1200KV BLDC motor was the limiting factor; preliminary tests with a 13×6.5 propeller caused significant overheating around 3500 Revolutions per minute (RPM). Therefore, for this specific setup, 10×5-inch propellers or smaller ones are proposed. A key feature is the instrument's modular design, allowing the BLDC motor to be easily exchanged for a more powerful unit to accommodate larger thrust loads. The technical specifications of each electronic component used in the fabrication of the test stand are detailed in Table I.

TABLE I. TECHNICAL SPECIFICATIONS OF KEY COMPONENTS

Component	Brand	Key specifications	Function in the system
Microcontroller	ESP32	32-bit dual-core, integrated Wi-Fi and bluetooth, analog-to-digital converter (ADC)	Central data acquisition processes signals from all sensors
BLDC motor	A2212	1200 KV, recommended for 3S LiPo	Provides rotational power to drive the test propellers
ESC	Hobbywing Skywalker	50 A continuous current, 2-4 S LiPo compatible	Regulates motor speed based on the Pulse Width Modulation (PWM) input signal
Thrust sensor	TAL220 5 kg beam load cell	5 kg maximum capacity	Measures the static thrust force generated by the propeller
Sensor amplifier	HX711 Module	24-bit ADC for high precision	Amplifies and digitizes the analog signal from the load cell
Power sensor	Astro Flight wattmeter	100A capacity. Measures real-time voltage (V), current (A), and power (W)	Provides measurement of the electrical power consumed by the system
Airflow velocity sensor	Krisbow environment meter 5 in 1	Measures air speed in m/s. Manufacturer-stated accuracy of ±3% of reading	Quantifies the exit airflow velocity from the propeller
RPM sensor	DT-2234C+ (Digital Laser Tachometer)	3.3 V-5 V logic level, Digital pulse output, Slotted IR optocoupler. High accuracy of ± (0.05% + 1 digit)	Measures rotational speed of the propeller and provides pulse data to the microcontroller
Power Source	3S LiPo battery	11.1 V Nominal voltage, 5200 mAh capacity	Supplies electrical energy to the entire test system
Control Input	Manual servo tester	Generates a standard PWM signal (1000-2000 μs)	Provides a stable and repeatable throttle signal to the ESC for testing

The electronic architecture was designed for simultaneous, reliable data acquisition, centered around an ESP32 microcontroller. This microcontroller was chosen for its dual-core processor and integrated ADC, allowing it to efficiently manage data streams from multiple sensors. The measurement system relies on integrating key sensors. For thrust measurement, a beam-type load cell is paired with an HX711 24-bit amplifier. This module digitizes the high-resolution analog signal, providing a stable, noise-resistant digital feed. Simultaneously, an Astro Flight wattmeter provides real-time power metrics (voltage, current, and power), while a Krisbow Environment Meter 5 in 1 quantifies outflow air velocity. A manual servo tester provides a stable PWM control signal to the ESC. This was a deliberate design choice to isolate the control input from the microcontroller's main loop. This ensures that the throttle command is exceptionally stable and repeatable, removing potential signal jitter. This integrated, multi-sensor architecture ensures that all parameters used for efficiency calculation, as obtained in (5), are captured synchronously. The electronic configuration is illustrated in Figure 3.

### B. System Assembly and Calibration

Following assembly, a comprehensive calibration and verification process was conducted to ensure the accuracy and reliability of the integrated sensor suite. Particular attention was given to the thrust measurement system, utilizing a TAL220 5kg beam load cell and the HX711 24-bit amplifier. A static calibration was performed using standard laboratory weights applied in increments from 0 to 1000 g. The raw ADC output data from the HX711 were recorded for each load increment. The resulting calibration curve is displayed in Figure 4.

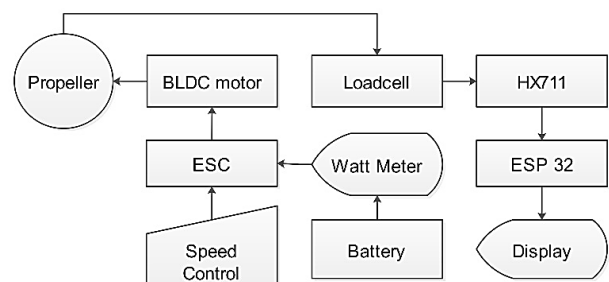


Fig. 3. Schematic of the electronic architecture.

The data demonstrates a strong linear relationship between the applied mass (x-axis) and the sensor output (y-axis). Linear regression analysis yielded the calibration equation:

$$y = 879.63x + 35.784$$

where  $x$  is the applied mass in g, and  $y$  is the corresponding raw ADC output. This analysis produced a coefficient of determination ( $R^2$ ) of 0.98. This strong  $R^2$  value confirms the high linearity and measurement accuracy of the system, indicating that 98% of the data variation is explained by the linear model. The equation was subsequently embedded into the ESP32 firmware to convert raw ADC values into precise thrust readings in g (which were then converted to N for analysis).

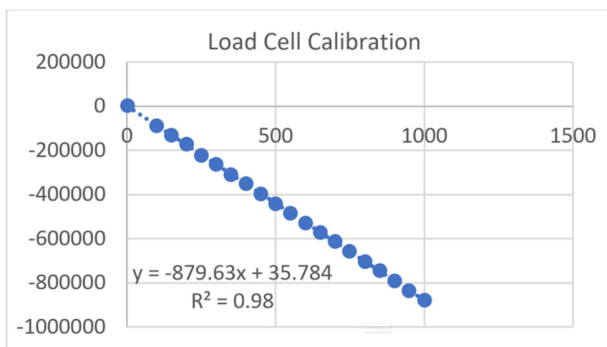


Fig. 4. Load cell calibration curve.

The other commercial off-the-shelf instruments were factory-calibrated devices selected for their high accuracy. The Astro Flight Wattmeter 100A was used to record electrical power, providing high-resolution measurements (0.01V, 0.01A). For measuring exit airflow velocity, a Krisbow Environment Meter 5 in 1 was employed. This multifunctional device, utilizing its digital vane anemometer component, has a manufacturer-stated velocity accuracy of  $\pm 3\%$  of reading. Finally, non-contact RPM measurement was performed using a DT-2234C+ digital laser tachometer, featuring a high accuracy of  $\pm (0.05\% + 1 \text{ digit})$ . To facilitate stable readings, a piece of reflective tape was applied to the propeller hub for each test.

### C. Experimental Subjects

To validate the instrument's sensitivity and analytical capabilities, three propellers with identical geometric designs (10-inch diameter and 5-inch pitch) were used as test subjects. This allowed for the isolation of performance variations caused solely by different manufacturing methods. The first propeller, as shown in Figure 5, serving as the performance benchmark, was a commercial product made from hard plastic via industrial injection molding.

The second propeller was independently fabricated using a casting method. This involved creating a silicone mold from the commercial propeller and then casting the final part using a polymer resin. The resulting cast propeller is portrayed in Figure 6. The third propeller, as depicted in Figure 7, was manufactured employing FDM 3D printed technology with PLA material, matching the material used for the test stand frame.



Fig. 5. Commercial propeller.



Fig. 6. Casting propeller.



Fig. 7. 3D Printed propeller.

### D. Experimental Protocol and Data Collection

The experiments were conducted by securing each of the three propellers to the BLDC motor on the test stand. To compare their performance, each propeller was tested at three distinct and stable throttle settings, controlled by specific PWM signals: 1028  $\mu\text{s}$  (low throttle), 1204  $\mu\text{s}$  (medium throttle), and 1330  $\mu\text{s}$  (high throttle). The use of fixed PWM signals as the independent variable, rather than fixed RPMs, was a deliberate methodological choice. This approach directly simulates real-world UAV operation, where the flight controller issues a specific PWM command to the ESC. The resulting motor RPM, thrust, and power consumption are dependent variables characterizing the total system's response to that command. This method allows for a holistic performance comparison, answering the practical engineering question of which assembly provides the most efficient conversion of electrical power to thrust for the same control input. While testing at constant RPMs is valid for pure aerodynamic component analysis, testing at constant PWM input provides a more accurate measure of the overall propulsion system's practical efficiency, the main focus of this study. For each PWM test point, the system was allowed to run until all sensor readings were stable, and the representative, stable values were then recorded for analysis.

To quantify the instrument's measurement error and validate its repeatability, a dedicated repeatability test was conducted separately. The system was run using the commercial propeller at a fixed medium throttle (1204  $\mu\text{s}$ ) and allowed to thermally stabilize for 10 min, after which 20 consecutive data points were recorded from the instrument. Statistical analysis of these stable-state data confirmed the instrument's high precision, yielding a Relative Standard Deviation (RSD) of 1.1% for thrust and 0.8% for RPM measurements, a low error margin that validates the reliability of the test bench for capturing the representative data illustrated in Table II.

### E. Analytical Framework and Performance Metrics

The analytical framework for performance measurement is based on quantifying the total efficiency ( $\eta_{total}$ ) of the propulsion system, which represents the system's overall effectiveness in converting input electrical power into useful aerodynamic thrust power. The total efficiency is a product of

its two main components: motor efficiency ( $\eta_m$ ) and propeller efficiency ( $\eta_p$ ).

$$\eta_{total} = \eta_m \times \eta_p \quad (1)$$

where motor efficiency ( $\eta_m$ ) is defined as the ratio of the mechanical power output delivered by the motor shaft to the electrical power it consumes. Electrical power is the product of the input voltage ( $V$ ) and current ( $I$ ), while the mechanical power is the product of the motor's torque ( $\tau$ ) and its angular velocity ( $\omega$ ).

$$\eta_m = \frac{\tau \cdot \omega}{V \cdot I} \quad (2)$$

where propeller efficiency ( $\eta_p$ ) is defined as the ratio of the useful thrust power generated to the mechanical power it receives from the motor shaft. The thrust power is the product of the generated thrust ( $T$ ) and the axial airflow velocity ( $v$ ).

$$\eta_p = \frac{T \cdot v}{\tau \cdot \omega} \quad (3)$$

To obtain a practical formula for total efficiency based only on directly measurable quantities, the expressions for motor and propeller efficiency are substituted into the (1) for calculating total efficiency:

$$\eta_{total} = \eta_m \times \eta_p = \left( \frac{\tau \cdot \omega}{V \cdot I} \right) \times \left( \frac{T \cdot v}{\tau \cdot \omega} \right) \quad (4)$$

The intermediate term for mechanical power  $\tau \cdot \omega$ , which is difficult to measure directly, appears in both the numerator and the denominator. This allows the term to be mathematically eliminated, resulting in a simplified equation for calculation of total propulsion efficiency, used in this study.

$$\eta_{total} = \frac{T \cdot v}{V \cdot I} \quad (5)$$

where each variable corresponds to a direct and simultaneous measurement from the instrument's sensor array:  $T$  is the thrust (N) measured by the load cell,  $v$  is the axial airflow velocity (m/s) measured by the anemometer, and  $V$  and  $I$  are the input voltage (V) and current (A) measured by the wattmeter.

### III. RESULT AND DISCUSSION

#### A. Fabricated Instrument and Direct Experimental Measurements

The development phase culminated in the successful fabrication of the fully functional, integrated test stand, as shown in Figure 8. The instrument, securely assembled on a rigid wooden base, effectively houses all mechanical and electronic components, thereby validating the design and fabrication process detailed in the methodology.

The instrument was subsequently utilized in a validation study on the three 10x5-inch propellers. Following the protocol described in the methodology, the instrument directly measured primary operational parameters at three distinct and stable throttle settings, controlled by specific PWM signals: 1028  $\mu$ s, 1204  $\mu$ s, and 1330  $\mu$ s. The complete set of averaged, directly measured data from these experiments, including RPM, thrust, voltage, and current, is presented in Table II.

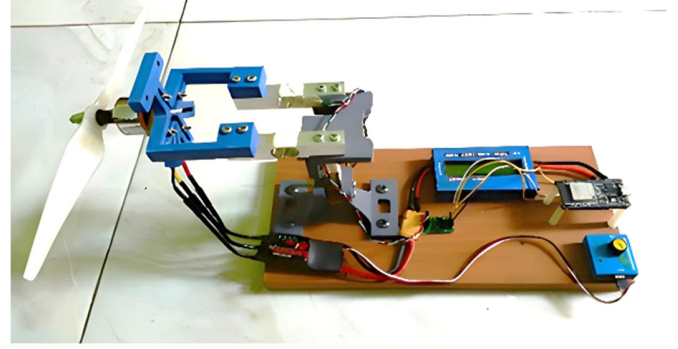


Fig. 8. Test instrument with mechanical and electronic subsystems.

TABLE II. EXPERIMENTAL MEASUREMENTS FROM THE TEST INSTRUMENT

Propeller	PWM signal ( $\mu$ s)	RPM	Thrust (N)	Voltage (V)	Current (A)
Commercial	1028	3743.7	0.66	11.20	2.07
	1204	5653.2	1.74	10.58	6.30
	1330	6373.9	2.21	10.00	10.29
Casting	1028	4105.8	0.73	11.22	2.46
	1204	5948.4	1.32	10.96	5.72
	1330	6934.5	1.92	10.61	9.13
3D printed	1028	4139.8	0.71	12.05	2.13
	1204	6040.3	1.63	11.61	6.87
	1330	6993.1	2.15	11.25	9.82

#### B. Performance Metric Calculation

Using the primary, directly-measured experimental data as presented in Table II, the key performance metrics were calculated to enable a comparative efficiency analysis. This data processing stage converts the raw sensor outputs into normalized Figures of Merit (FoM), allowing a direct comparison of the propeller manufacturing methods.

The first calculated metric was the input electrical power ( $P_{elec}$ ), determined from the product of the measured voltage ( $V$ ) and current ( $I$ ). This value represents the total power drawn from the 3S LiPo battery and serves as the primary "cost" component in (5), quantifying the total energy resource consumed by the entire system.

Simultaneously, the output thrust power ( $P_{thrust}$ ) was calculated, as defined by the analytical framework in (5). This value is the product of the measured thrust ( $T$ ) and the measured exit airflow velocity ( $v$ ). This metric represents the actual useful aerodynamic work (power, in W) being performed, a calculation vital for converting the static force (thrust) into a power unit that can be directly compared against the input electrical power.

Finally, the most important metric of this study, the total propulsive efficiency ( $\eta_{total}$ ), was calculated. This metric is the direct ratio of the output thrust power ( $P_{thrust}$ ) to the input electrical power ( $P_{elec}$ ), expressed as a percentage. This final, dimensionless value is the most crucial calculated metric, quantifying the overall effectiveness of the entire energy conversion chain, and providing a single, holistic benchmark to compare the practical performance of each propeller assembly.

The complete set of calculated performance metrics for each test condition is detailed in Table III.

TABLE III. CALCULATED PERFORMANCE METRICS FOR EACH PROPELLER

Propeller	PWM signal (μs)	Electrical power (watt)	Velocity (m/s)	Thrust power (W)	η Propulsion (%)
Commercial	1028	23.18	8.58	5.66	24.43%
	1204	66.65	11.62	20.22	30.33%
	1330	102.90	13.01	28.75	27.94%
Casting	1028	27.60	6.62	4.83	17.51%
	1204	62.69	9.79	12.92	20.61%
	1330	96.87	13.06	25.08	25.89%
3D Printed	1028	25.67	6.48	4.60	17.93%
	1204	79.76	10.39	16.94	21.23%
	1330	110.48	12.31	26.47	23.96%

C. Comparative Performance Analysis and Discussion

The data presented in Table III illustrate significant performance differences among the propellers based on their manufacturing method. The commercial propeller consistently demonstrated superior performance, achieving the highest total propulsive efficiency at all test points and reaching a peak efficiency of 30% at a 1204 μs PWM signal. This superior performance suggests that its high-dimensional accuracy and smooth surface finish result in a more efficient energy conversion. The comparative efficiency trends are visualized in Figure 9.

In contrast, both the 3D-printed and casting propellers showed notably lower efficiencies. Although the 3D-printed propeller was capable of producing high thrust (2.15 N), it was the least efficient in terms of power consumption, drawing the highest electrical power (110.48 W) at the 1330 μs setting. This inefficiency is likely due to surface imperfections, such as the characteristic layer lines of the FDM process, which increase aerodynamic drag.

Deeper analysis indicates two primary factors. The first is surface roughness. The 3D-printed propeller, despite being geometrically accurate, possesses characteristic FDM layer lines, which significantly increase turbulence and parasitic drag, directly degrading efficiency. The casting propeller, while smoother than FDM, cannot perfectly replicate the flawless injection-molded surface and likely possesses a different micro-texture, contributing to increased drag.

The second factor is material properties (blade rigidity and balance). The different materials (PLA, polymer resin, and hard commercial plastic) have varying densities and rigidity. This difference affects mass distribution (balance) as well as deformation and flexing of the blades under torsional load during rotation. Less rigid or improperly balanced blades can lead to vibrations or energy loss through deformation, further reducing propulsive efficiency.

These results are consistent with the expectations for non-ideal, real-world components tested under static conditions. While highly optimized systems can achieve efficiencies over 70% in simulations, the measured peak of 30% is a realistic benchmark for off-the-shelf and custom-fabricated

components. The ability of the developed instrument to accurately quantify this efficiency gap is a key finding, highlighting the trade-off between manufacturing accessibility and aerodynamic performance.

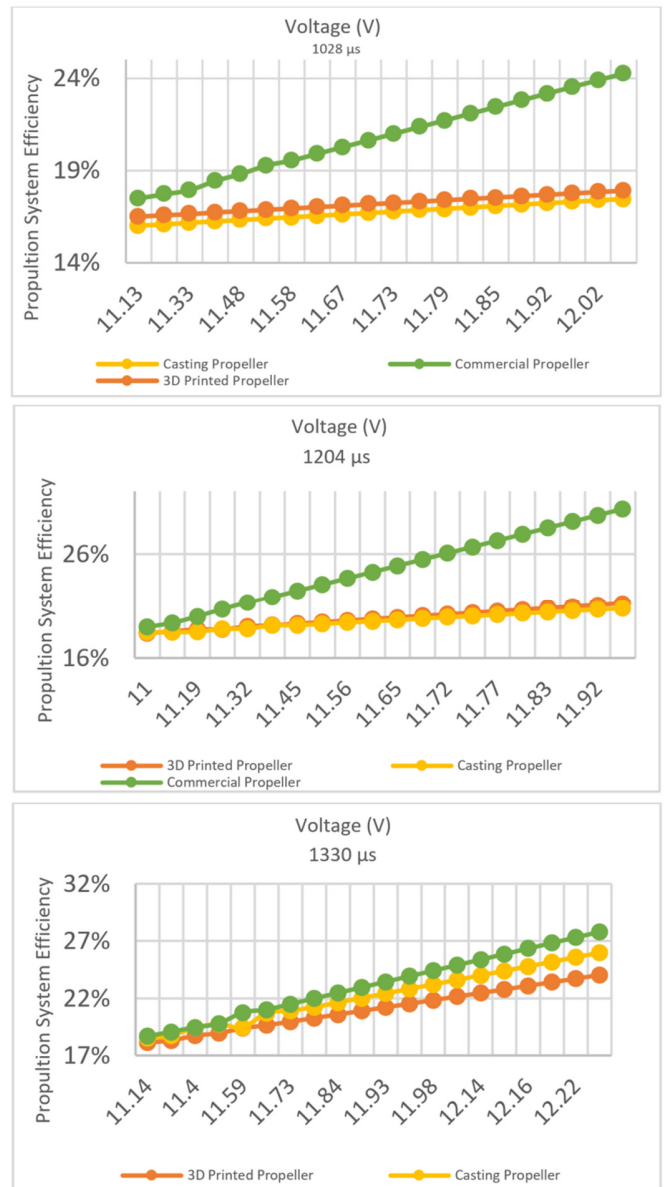


Fig. 9. Comparative propulsive efficiency of commercial, casting, and 3D printed propellers at 1028 μs, 1204 μs, and 1330 μs PWM signals.

The most significant implication of this work is the validation of the test instrument itself. The results demonstrate that the developed microcontroller-based system possesses the required sensitivity to distinguish clear, repeatable performance differences are due to subtle manufacturing variations, directly addressing the need for accessible analysis tools in research and education. Furthermore, the developed test instrument's ability to empirically identify a peak efficiency point (e.g., 30% at 1204 μs for the commercial propeller) provides actionable

data for optimizing UAV flight endurance. This demonstrates that the instrument is a valuable engineering tool for detailed system characterization, rather than merely a data-logging device.

#### IV. CONCLUSIONS

This study has successfully designed, fabricated, and validated a microcontroller-based test bench for the precise measurement of thrust and efficiency in electric propulsion systems. The functional validation of this test bench was demonstrated through a comparative analysis of three propeller types: commercial, casting, and 3D printed. The instrument proved highly efficient in measuring distinct performance differences, demonstrating that the commercial propeller achieved superior performance with a peak efficiency of 30% at a 1204  $\mu$ s PWM signal, owing to its smooth surface finish. The test bench also successfully identified the inherent inefficiencies of the 3D-printed propeller caused by Fused Deposition Modeling (FDM) layer lines. The ability of this custom-built system to produce repeatable and distinct measurements confirms its utility as a reliable tool for empirical research and development in Unmanned Aerial Vehicle (UAV) propulsion.

The successful design, fabrication, and validation of this test bench enable new opportunities for future research, such as enhancing the test bench itself by integrating additional sensors (e.g., for vibration or acoustic noise analysis) or broadening its software capabilities for real-time data visualization. Furthermore, the instrument enables broader investigations, such as testing propellers from advanced materials or analyzing the effects of post-processing techniques on custom-fabricated propellers. In terms of application, this microcontroller-based test bench serves as an accessible and effective platform for academic institutions to facilitate hands-on learning in mechatronics and aerodynamics. Moreover, it provides designers, engineers, and hobbyists with a critical tool to optimize component selection and enhance the overall efficiency of electric propulsion systems for various applications.

#### DATA AVAILABILITY STATEMENT

The data supporting the findings of this study are available from the corresponding author upon reasonable request.

#### ACKNOWLEDGMENT

The authors extend their sincere appreciation to the Direktorat Penelitian dan Pengabdian kepada Masyarakat (DPPM), Direktorat Jenderal Riset dan Pengembangan Kementerian Pendidikan Tinggi, Sains, dan Teknologi, for the financial support provided under 0498.38/LL5-INT/AL.04/2025, 001/VI/2025/STTKD.

#### REFERENCES

- [1] D. Joshi, D. Deb, and S. M. Mueen, "Comprehensive Review on Electric Propulsion System of Unmanned Aerial Vehicles," *Frontiers in Energy Research*, vol. 10, May 2022, Art. no. 752012, <https://doi.org/10.3389/fenrg.2022.752012>.
- [2] B. Zhang, Z. Song, F. Zhao, and C. Liu, "Overview of Propulsion Systems for Unmanned Aerial Vehicles," *Energies*, vol. 15, no. 2, Jan. 2022, Art. no. 455, <https://doi.org/10.3390/en15020455>.
- [3] O. D. Dantsker, R. Mancuso, M. S. Selig, and M. Caccamo, "High-Frequency Sensor Data Acquisition System (SDAC) for Flight Control and Aerodynamic Data Collection," in *32nd AIAA Applied Aerodynamics Conference*, Atlanta, GA, USA, June 2014, <https://doi.org/10.2514/6.2014-2565>.
- [4] O. Gur and A. Rosen, "Optimizing Electric Propulsion Systems for Unmanned Aerial Vehicles," *Journal of Aircraft*, vol. 46, no. 4, pp. 1340–1353, July 2009, <https://doi.org/10.2514/1.41027>.
- [5] M. Etewa, A. F. Hassan, E. Safwat, M. A. H. Abozied, M. M. El-Khatib, and A. Ramirez-Serrano, "Performance Estimation of Fixed-Wing UAV Propulsion Systems," *Drones*, vol. 8, no. 9, Aug. 2024, Art. no. 424, <https://doi.org/10.3390/drones8090424>.
- [6] N. S. Zawodny, H. Haskin, and D. M. Nark, "Aerodynamic Performance and Acoustic Measurements of a High-Lift Propeller in an Isolated Configuration," in *2018 AIAA/CEAS Aeroacoustics Conference*, Atlanta, GA, USA, June 2018, <https://doi.org/10.2514/6.2018-3448>.
- [7] P. Kósa *et al.*, "Experimental Measurement of a UAV Propeller's Thrust," *Tehnicki vjesnik - Technical Gazette*, vol. 29, no. 1, Feb. 2022, <https://doi.org/10.17559/TV-20201212185220>.
- [8] A. Alikhani and M. R. Salimi, "Design, Construction and Performance Evaluation of a Cold Gas Thruster Test Stand," *Journal of Space Science and Technology*, vol. 15, no. English Special Issue, pp. 55–64, Mar. 2022, <https://doi.org/10.30699/jsst.2021.1305>.
- [9] T. H. Stevenson and E. G. Lightsey, "Design and Operation of a Thrust Test Stand for University Small Satellite Thrusters," in *2018 AIAA Aerospace Sciences Meeting*, Kissimmee, FL, USA, Jan. 2018, <https://doi.org/10.2514/6.2018-2117>.
- [10] Z. Jun, M. A. Akbar, W. Xin Lei, C. Yi Hua, and Danaish, "Theoretical and experimental investigation of six-degree-of-freedom force/thrust measurement stand," *IET Science, Measurement & Technology*, vol. 14, no. 8, pp. 883–890, Oct. 2020, <https://doi.org/10.1049/iet-smt.2020.0046>.
- [11] M. R. Inchingolo, M. Merino, M. Wijnen, and J. Navarro-Cavallé, "Thrust Measurements of a Waveguide Electron Cyclotron Resonance Thruster," *Journal of Applied Physics*, vol. 135, no. 9, Mar. 2024, Art. no. 093304, <https://doi.org/10.1063/5.0186778>.
- [12] M. Kühn, C. Toursel, and J. Schein, "Thrust Measurements on the High Efficient and Reliable Vacuum Arc Thruster (HERVAT)," *Applied Sciences*, vol. 11, no. 5, Mar. 2021, Art. no. 2274, <https://doi.org/10.3390/app11052274>.
- [13] H. Wang, W. Wang, J. Yan, C. Fu, and W. Liu, "Measurement and Prediction of Micronewton Class Thrust of Electric Propulsion Based on the Torsional Pendulum and Machine Learning Technique," *IEEE Transactions on Instrumentation and Measurement*, vol. 72, pp. 1–14, 2023, <https://doi.org/10.1109/TIM.2022.3225035>.
- [14] A. Pugna, C. Hrab, L.-N. Hînsa, A. Hopârtean, C.-M. Giurgea, and L. Marcu, "Development of an Experimental Setup for Propeller Performance Measurements," *E3S Web of Conferences*, vol. 608, 2025, Art. no. 02013, <https://doi.org/10.1051/e3sconf/202560802013>.
- [15] C. Singh, R. Samkaria, and T. Shukla, "Propeller Power Effect Study Instrumentation for Performance Evaluation of Aircraft Design," in *2020 IEEE 17th India Council International Conference*, New Delhi, India, Dec. 2020, pp. 1–5, <https://doi.org/10.1109/INDICON49873.2020.9342502>.
- [16] S. Scharmann *et al.*, "Thrust Measurement of an Ion Thruster by a Force Probe Approach and Comparison to a Thrust Balance," *AIP Advances*, vol. 12, no. 4, Apr. 2022, Art. no. 045218, <https://doi.org/10.1063/5.0066401>.
- [17] Drone Building and Optimization: How to Increase Your Flight Time, Payload and Overall Efficiency. Gatineau, QC Canada: Tyto Robotics, 2025.
- [18] *Series 1585 Thrust Stand*. (v. 2025), Tyto Robotics, Gatineau, QC Canada. [Online]. Available: <https://www.tytorobotics.com/pages/series-1580-1585>.

## AUTHOR PROFILES

**Erwan Eko Prasetyo** received the B.S. degree from the Universitas Negeri Yogyakarta (UNY), Yogyakarta in 2012 and the M.Eng. degree from the Universitas Gadjah Mada, Yogyakarta in 2015, both in electrical engineering. His research interests include electronics, microcontroller, artificial intelligence, and internet of things.

**Erwhin Irmawan** earned his Bachelor's, Master's, and Doctoral degrees from Universitas Gadjah Mada (UGM), Indonesia, specializing in Electronics and Instrumentation. His research interests include aerospace control systems, UAV instrumentation, and autonomous flight stability.

**Gaguk Marausna** received the B.S. degree in mechanical engineering from Universitas Muhammadiyah Malang and the M.S. degree in mechanical engineering from Universitas Gadjah Mada, Yogyakarta, in 2019. His research interests include energy conversion, heat transfer, and aerodynamics.

**Hendriana Helda Pratama** received the B.S. degree from Universitas Ahmad Dahlan (UAD), Indonesia in electrical engineering. He is currently pursuing the M.S. degree with the Master Program of Electrical Engineering, Universitas Ahmad Dahlan (UAD), Indonesia. His research interests include artificial intelligence, computer vision, signal processing, and control system.

**Ikbal Rizki Putra** received the B.S. degree in Engineering in Mechanical Engineering Universitas Muhammadiyah Yogyakarta in 2015 and the Master degree in the Mechanical Engineering from Universitas Gadjah Mada. His research interest includes the 3D printed, product design and development.

**Fadhli Atha Hidayat** received his bachelor's degree in Aerospace Engineering from Sekolah Tinggi Teknologi Kedirgantaraan (STTKD), Yogyakarta, in 2025. His research interests include UAV, propulsion system, and electronic instrumentation.